Spin-polarized multi-photon photoemission and surface electronic structure of Cu(001)

2010 New J. Phys. 12 083022

(http://iopscience.iop.org/1367-2630/12/8/083022)

New Journal of Physics
The open-access journal for physics

Spin-polarized multi-photon photoemission and surface electronic structure of Cu(001)

W-C Lin[1,2], A Winkelmann[1,4], C-T Chiang[1], F Bisio[3] and J Kirschner[1]

[1] Max-Planck-Institut für Mikrostrukturphysik, Weinberg 2, D-06120 Halle (Saale), Germany
[2] Department of Physics, National Taiwan Normal University, Taipei 11677, Taiwan
[3] CNR-SPIN, Corso Perrone 24, I-16152 Genova, Italy
E-mail: winkelm@mpi-halle.mpg.de

New Journal of Physics **12** (2010) 083022 (13pp)
Received 4 March 2010
Published 10 August 2010
Online at http://www.njp.org/
doi:10.1088/1367-2630/12/8/083022

Abstract. We have investigated the influence of controlled modifications of the surface electronic structure of Cu(001) on the spin polarization of photoelectrons emitted via multi-photon excitation. Using ultrashort, circularly polarized laser pulses with $\sim$3 eV photon energy, spin-polarized electrons can be selectively excited from the spin–orbit (SO) coupled d-bands of Cu into the unoccupied $n = 1$ image potential (IP) state on the Cu(001) surface. Upon lowering the IP state energy level by submonolayer Cs deposition, we show that the IP energy can be tuned into two-photon resonance with initial state d-bands of different double group symmetry, leading to a sign reversal of the spin polarization that is observed at the IP state level. Similarly, exploiting the parallel-momentum IP state dispersion, the resonant tuning of the IP state energy level to different branches of the SO split d-bands is demonstrated. Our results highlight the role of resonant and off-resonant excitation pathways in determining the spin polarization in the excited states. The additional information contained in spin-resolved multi-photon photoemission experiments can be exploited to obtain insights into the mechanism of population of excited states.

[4] Author to whom any correspondence should be addressed.

Contents

1. Introduction

Spin-resolved photoemission is a powerful tool for the analysis of the relativistic electronic band structure on surfaces [1, 2]. In the presence of spin–orbit coupling (SOC) in the electronic structure, circularly polarized light can be utilized to selectively excite spin-polarized electrons in nonmagnetic materials [3]–[10]. The extension of this approach to nonlinear photoemission using ultrashort laser pulses for excitation offers the possibility to optically control spin-dependent excitation processes of electrons into unoccupied states at nonmagnetic surfaces [11, 12]. Similarly, access to unoccupied states and to dynamical spin-dependent scattering processes at magnetic surfaces can be gained via two-photon photoemission in spin-resolved pump-probe experiments [13]–[15].

In previous studies, we demonstrated the control over the spin polarization of the excited photoelectrons at a Cu(001) surface by fine-tuning the excitation photon energy [11, 12], exploiting the efficient multi-photon resonant coupling between the SO-split Cu d-bands and the unoccupied $n = 1$ image-potential (IP) state [16]. This can be seen in figure 1(a), where we show a simplified level scheme derived from the relativistic Cu(001) band structure shown in detail in figure 3. The unique combination of efficient resonant multi-photon photoemission and the possible spin-selective photoexcitation by circularly polarized light makes the Cu(001) surface a highly interesting and well-defined model system for further investigations. As the resonant excitation pathways are highly k-space selective and magnetism-induced spin relaxation channels are absent, the nonmagnetic Cu(001) surface is particularly suited to investigating the specific details of the buildup and decay of spin-polarized electron populations. Spin-polarized electrons can in fact be effectively 'labelled' by their own spin orientation, thereby providing clues to their initial state and their decay path that would be more difficult to obtain otherwise. In this respect, extending our knowledge of different mechanisms of creating and manipulating excited spin populations at nonmagnetic surfaces represents an interesting issue.

Besides the experiments mentioned above, in which the spin polarization of the photoemitted electrons is tuned by acting on the characteristics of the incident excitation light, alternative approaches are available to influence the electron spins. They involve, for instance, the controlled manipulation of the intermediate states in a multi-photon process in order to influence their resonant light-induced coupling with the SO-split initial states.

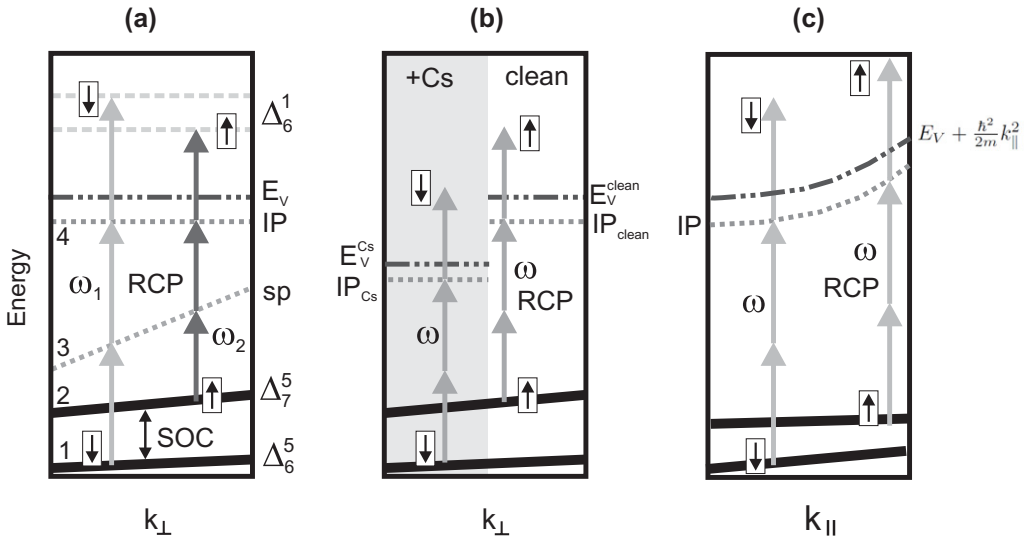

Figure 1. Simplified level schemes for tuning the excited spin polarization at Cu(001) by different approaches (compare with figure 3 for the numbering of the bands). Previous work: (a) tuning of the photon energy from ω_1 to ω_2 [11, 12]. This work: (b) tuning of the IP state level by workfunction reduction (vacuum level E_V) under Cs adsorption in normal emission; (c) using the IP state level dispersion with $k_\parallel$ in off-normal emission (only electrons with energies larger than $E_V + (\hbar^2/2m)k_\parallel^2$ can overcome the surface barrier). The initial occupied d-band of Δ^5 spatial symmetry is split by SOC into the two relativistic Δ_6^5 and Δ_7^5 symmetries. The optical selection rules are shown for right-circular polarized (RCP) light.

In this paper, we report the results we obtained applying two such different methods for tuning the spin polarization of electrons photoemitted in a multi-photon process from Cu(001). The methods are illustrated in figures 1(b) and (c). The first approach (figure 1(b)) consists in tuning the energy level of the $n = 1$ IP state to control the resonance conditions with the SO-split initial states via the deposition of a submonolayer Cs coverage on the Cu(001) surface. The second approach (figure 1(c)) is to exploit the free-electron-like dispersion of the $n = 1$ IP state as a function of surface-parallel momentum $k_\parallel$ [16] to achieve resonant coupling with the d-bands off the surface Brillouin zone (BZ) centre. The results obtained following these two approaches are compared with corresponding available data obtained by one-photon photoemission [10] or spectroscopic multi-photon photoemission [11], allowing us to assess the influence of the different excitation pathways and the characteristics of the intermediate states on the final-state spin polarization.

2. Experiment

The experiments were carried out in an ultrahigh vacuum (UHV) system described previously in [11, 16]. A sketch of the experimental setup is shown in figure 2. Ultrashort laser pulses ($<$20 fs) with photon energy tuneable in the range $h\nu = 3.00$–3.15 eV were provided by the frequency-doubled output of a self-built Ti:sapphire oscillator. Right- and left-circular

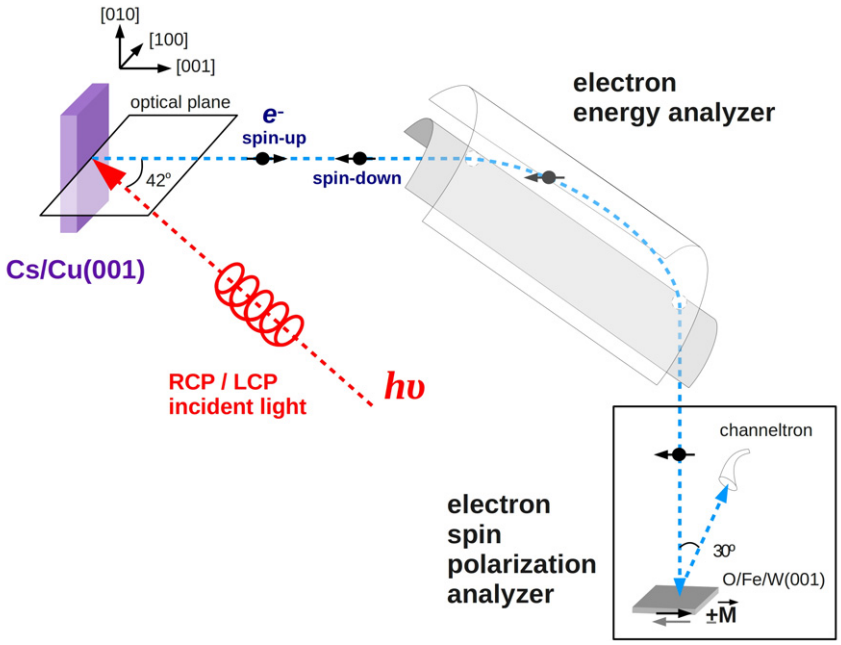

Figure 2. The experimental setup.

polarization (RCP and LCP) could be set by a combination of achromatic $\lambda/4$ and $\lambda/2$ wave plates. After cycles of sputtering and annealing, a clean and well-ordered Cu(001) surface was prepared. Caesium (Cs) was deposited on Cu(001) at a background pressure lower than 5×10^{-10} mbar from a commercial getter source (SAES). The optical plane was aligned parallel to the [100] Cu direction. The photoemission spectra were measured by a cylindrical sector analyser (Focus CSA300, energy resolution 150 meV, angular resolution $\approx 3^\circ$) coupled to a spin detector based on exchange scattering at a magnetic Fe thin film [17]. For the normal-emission measurements, the spin component perpendicular to the Cu(001) surface was analysed [9]. For off-normal emission measurements, the sample was rotated about the axis normal to the optical plane while keeping the angle between the incident laser beam and the collection axis of the electron analyser constant (42°). The orientation of the magnetization vector in the spin detector was kept unchanged with respect to the normal emission case (see below).

3. Results

3.1. Three-photon photoemission (3PPE) from Cs/Cu(001)

The general mechanism for the multi-photon coupling between d-bands and IP state in normal emission [16, 18] is illustrated in figure 3, where we show the relativistic Cu bulk band structure along the [001] surface normal direction (Γ to X) [19] together with the positions of the $n = 1$ IP state [20] and a relatively broad unoccupied surface resonance observed by inverse photoemission [21]. The vertical lines indicate a possible resonant condition for 3PPE for photon energies around 3 eV, coupling the SO-split d-bands with the IP state (the separation of the d-bands is about $\Delta E_{so} \approx 150$ meV [10]). A simplified close-up view of the energy levels involved is shown in figure 1(a). According to the relativistic optical selection rules in the

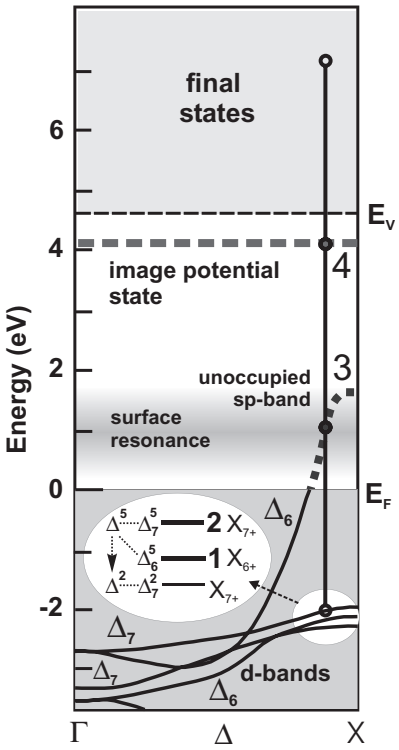

Figure 3. Relativistic band structure of Cu(001) along the Δ line, with possible resonant 3PPE excitation pathways for $h\nu \sim 3$ eV indicated by the vertical lines.

presence of SOC in the Cu d-bands, spin-polarized electrons can be resonantly excited from Δ_6 or Δ_7 d-bands, through the intermediate unoccupied sp-band, and the $n = 1$ IP state [22].

If the photon energy is such as to resonantly couple the upper d-band branch with the IP state on the clean surface, then lowering the IP state energy by an amount similar to ΔE_{so} should result in resonant coupling with the lower d-band branch. Accordingly, this should result in a sign reversal of the 3PPE spin polarization excited via the IP state (compare with figure 1(b)). Since the IP state level intrinsically correlates with the position of the vacuum level E_V, it is straightforward to consider the tuning of the vacuum level by lowering the workfunction by means of Cs deposition [23, 24].

In figure 4, we show the spin-resolved measurements of the 3PPE IP peak with photon energy $h\nu = 3.05$ eV for two Cs coverages. The Cs deposition and the measurements were performed at 300 K. The energy scale refers to the Fermi level E_F. The Cs coverage is calibrated from the workfunction value extracted from the low-energy cutoff of the spectra (not shown) [25, 26], with 1 monolayer (ML) containing 4.12×10^{14} atoms cm^{-2}, corresponding to the saturation coverage of Cs/Cu(001) [26]. Upon 0.022 ML Cs deposition, the workfunction is lowered from 4.6 to 4.3 eV, whereas the 3PPE final state is shifted downwards by 0.1 eV. The different energy shift of the vacuum level and of the IP state has also been observed previously [25, 26] and was ascribed to the influence of the local positive electric field produced by the Cs ions on the Cu(001) surface [23], [27]–[29].

In the graph panels, the spin-up (spin-down) spectra measured by LCP radiation are reported as black dotted (solid) lines. The corresponding spin polarization spectra are reported

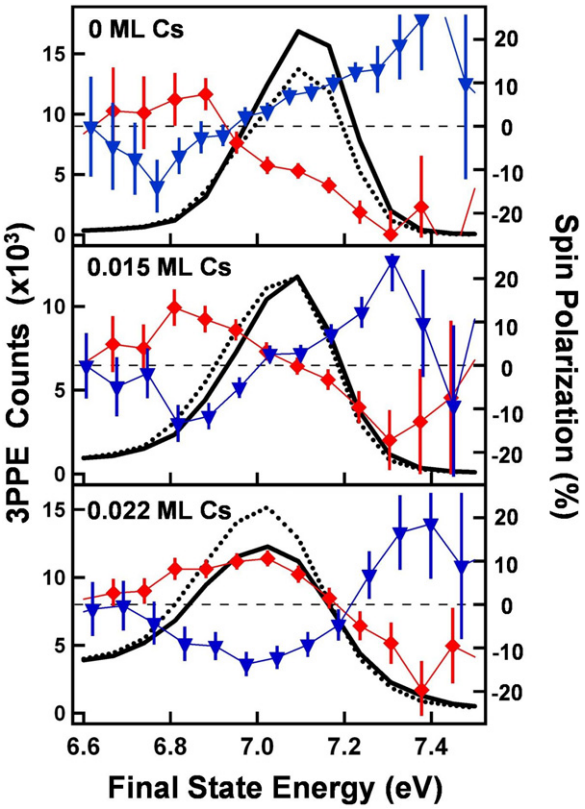

Figure 4. Spin-up (dotted lines) and spin-down (solid lines) spectra measured with LCP light for different Cs coverages on Cu(001). Photon energy $h\nu = 3.05$ eV. The symbols ▼ and ♦ indicate the corresponding spin polarization obtained from the measured spectra excited by RCP and LCP light, respectively. The lines are a guide to the eye.

as red diamonds. The blue triangles refer to RCP light, for which the spin polarization reverses its sign according to selection rules. In accordance with the IP state peak maximum, the 3PPE spin polarization gradually evolves from +8% on the clean Cu(001) to 0% at 0.015 ML Cs and then changes sign to reach −11% at 0.022 ML Cs/Cu(001), in agreement with the expected switch of resonant coupling from the upper to the lower branch of the d-band initial states. Besides the sign reversal in accord with the peak IP intensity, we notice that the spin-polarization spectra do not retain a constant shape when the excitation conditions are changed (i.e. the zero crossings do not stay at a constant energy). This effect we will address in the discussion. The further increase in the Cs coverage beyond the values addressed in the measurements shown here causes a marked broadening of the IP state peak accompanied by a strong decrease in its intensity, which prevented spin-resolved 3PPE measurements with sufficient statistics.

3.2. Angle-dependent 3PPE

Moving away from the normal emission condition, the free-electron-like $k_{\|}$-dispersion of the IP $n = 1$ energy level on Cu(001) in principle provides another method to modulate the 3PPE spin polarization [16]. In this case, it is the upward IP level shift with increasing $k_{\|}$ that provides

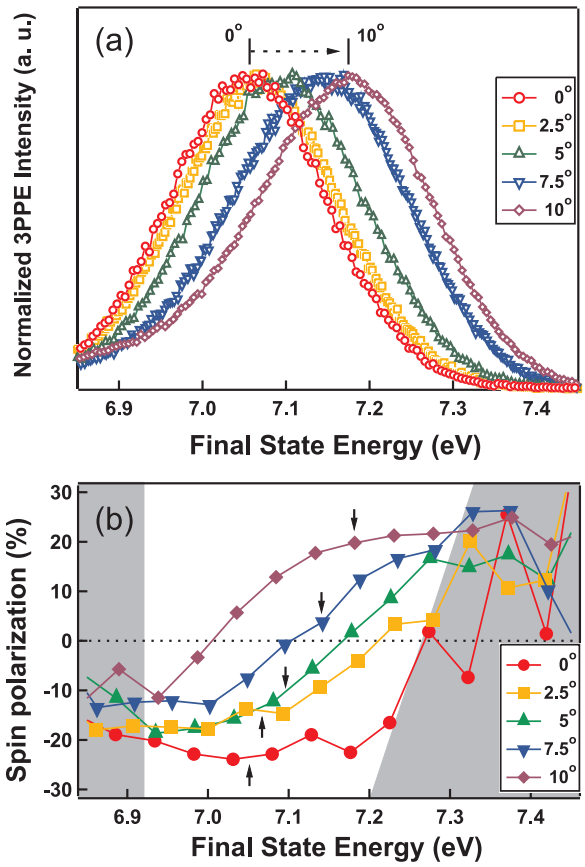

Figure 5. (a) Spin-integrated 3PPE spectra recorded at emission angle 0°–10° relative to the surface normal with 3.11 eV photon energy. The spectra are normalized to their maximum to allow for a better comparison. (b) Spin-polarization spectra as a function of the emission angle for RCP excitation. The arrows point to the corresponding IP maximum intensity as deduced from (a). The error bar of spin polarization near the 3PPE resonance peak is within ±2%. In the grey area, the error bars are larger than ±3%.

a variable-energy intermediate level which can couple with either of both SO-split initial state bands (compare with figure 1(c)). Despite the apparent similarity with respect to the previous method, several differences are expected. In order to achieve a variation in the IP state energy, it is necessary to measure the spectra under off-normal conditions, yet at a value of $k_{\parallel}$ for which the two-photon coupling between d-bands and IP state is still significant. This implies that also the initial d-band states will not be located along the ΓX line, so that their symmetry character and SO splitting can in principle differ with respect to the normal emission case (this is also symbolized by the slightly changed initial states in figure 1(c)).

In figure 5(a), we report a set of spin-integrated 3PPE spectra in the IP energy region measured with $h\nu = 3.11$ eV photon energy as a function of the off-normal emission angle θ. At $\theta = 10^{\circ}$ the 3PPE peak shifts upward by ~ 0.15 eV from 7.05 to nearly 7.2 eV, an energy shift of the order of ΔE_{so}. At $h\nu = 3.11$ eV and normal emission conditions, the IP state is resonantly coupled with the lower-energy branch of the SO-split d-bands at approximately -2.2 eV energy.

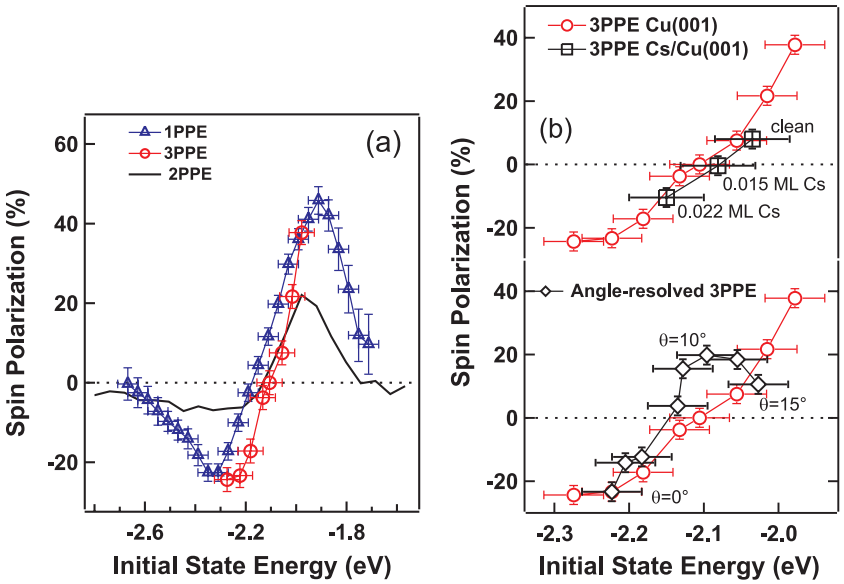

Figure 6. (a) Spin polarization as a function of initial state energy deduced by 1PPE (triangles) and 3PPE (circles). The results are adapted from [10, 11]. Black line: spin polarization as a function of initial state energy deduced by two-photon photoemission (2PPE) from Cs/Cu(001). (b, top) Spin polarization as a function of initial state energy for $h\nu = 3.05$ eV deduced from Cs coverage experiments (squares). The circles are 3PPE data from panel (a) reported for reference. (b, bottom) Spin polarization as a function of initial state energy for $h\nu = 3.11$ eV deduced from angle-dependent photoemission measurements. The circles are 3PPE data from panel (a) for reference.

For an increasing IP state energy level, the resonant coupling conditions will be met for initial states having also a correspondingly higher energy, so we expect to couple to the Δ_6 d-band, which is higher in energy. The spin polarization corresponding to each of these measurements is shown in figure 5(b), where the arrows point to the 3PPE peak position as deduced from figure 5(a). The 3PPE spin polarization at the peak maximum starts from -23% at $\theta = 0^\circ$, passes through zero at $\theta = 7.5^\circ$, and reaches the opposite sign of $+18\%$ at $\theta = 10^\circ$ emission angle, in general agreement with our schematic picture.

Again, we notice that the spin-polarization spectra show significant variation in their overall shape as a function of the excitation condition.

4. Discussion

In this section, we will address two aspects of the data. Firstly, this concerns the comparison of the spin polarization values reported in this investigation with reference data measured by angle-resolved one-photon photoemission (1PPE) [10] and with values obtained by photon-energy-dependent 3PPE [11]. Secondly, we assess the role of resonant excitation pathways in determining the full spin-polarization spectra in our multi-photon scheme.

In figure 6 (top panel), we plot the spin polarization of electrons photoemitted at normal emission from the SO-split Cu d-bands, as a function of their initial state energy measured in

1PPE (triangles) with $h\nu = 11$ eV excitation [10]. The spin polarization versus the initial state energy (deduced by subtracting from the final state energy the energy supplied by the photon excitation) reaches maximum values of +45 and −25% at −1.9 and −2.3 eV below the Fermi level, respectively. The circles in figure 6(a) represent the initial-state spin polarization deduced from the *resonant* IP state polarization in 3PPE experiments on clean Cu(001), measured by tuning the exciting photon energy $h\nu$ from 3.00 to 3.14 eV [11]. Here, the initial state energy was deduced from the final state energy by subtracting the energy supplied by the multi-photon (3PPE) excitation while considering the value corresponding to the *maximum IP state intensity* as the correct one for the spin polarization. Following this procedure, the 3PPE resonant spin polarization agrees well with 1PPE data in the region accessible by our experiments.

In the top part of figure 6(b), we report (black empty squares) the spin polarization as a function of the initial state energy deduced from the Cs-coverage-dependent measurements performed with $h\nu = 3.05$ eV excitation along with the reference 3PPE data from the clean surface (circles). The broadening and reduction of the IP state peak with Cs adsorption restrict the amount of Cs coverage that allows us to observe the resonant 3PPE [26, 30], thereby limiting the accessible initial-state range. Nevertheless, the spin polarizations in the initial state deduced via the two methods agree very well, as demonstrated by their strong overlap. This confirms that the physical picture underlying the idea of tuning the spin polarization in the IP state by shifting its energy level is essentially correct.

The spin polarization measured in the angle-dependent photoemission experiments reported in section 3.2 is shown in the bottom section of figure 6(b) for emission angles ranging from $\theta = 0^\circ$ to $\theta = 15^\circ$. Again, reference 3PPE data are reported for comparison. For small θ, the spin polarization is quantitatively similar to the reference normal-emission 3PPE result. The more the emission angle is increased, the more the discrepancies between the two sets of data increase. The spin polarization deduced via angle-resolved measurements reaches a maximum for $\theta \approx 10^\circ$ and then decreases for larger angles, and exhibits significantly different absolute values. These differences can be accounted for on the basis of a variety of phenomena taking place in off-normal emission geometry. Firstly, as mentioned previously, the d-band initial states for off-normal photoemission differ with respect to the ones at the $\overline{\Gamma}$ point shown in figure 3. The spin polarization measured in the experiment is accordingly determined by both the splitting and the exact binding energy of each SO split band as a function of $k_\parallel$. Whereas in the close proximity of the $\overline{\Gamma}$ point (small emission angle θ) we can safely assume minor changes, this assumption might not hold for the large θ case. Secondly, moving out from the normal emission case by an angle θ, the incidence angle of the circularly polarized laser beam gradually increases as $42^\circ + \theta$. Due to the different transmission coefficients of p-polarized and s-polarized light, the degree of ellipticity of the light (ϵ) in the interior of the material changes as a function of the incidence angle, decreasing from 0.64 at 42° incidence angle to 0.41 at 57° ($\epsilon = 1$ in vacuum) [31, 32]. The corresponding ratio of RCP to LCP components in light intensity is approximately 78 : 1 and 20 : 1 for 42° and 57° incident angle, respectively, possibly yielding a reduction in the electron spin polarization that can be quantified at 5% at the largest incidence angle. Finally, keeping a constant orientation of the detection direction in the spin detector will lead to a change to the measured spin polarization. In the absence of in-plane spin-polarization components, we expect a reduction in the spin polarization proportional to the cosine of the emission angle θ; therefore, this might be a minor effect in the θ range addressed here. All these effects are, by definition, irrelevant at normal emission, whereas their contribution gradually increases with increasing emission angle. This thereby justifies the observation that

the spin polarization measured by angle-resolved measurements agrees with reference data for normal emission and deviates from the expected behaviour the more the emission angle is increased.

The second point we address is the apparent change in the shape of the spin-polarization spectra as a function of the change in the $d \rightarrow$ IP resonance conditions induced by the tuning of the IP state energy. We focus on the Cs-dependent measurements. It is obvious that, when trying to deduce the initial-state spin polarization from each separate spectrum, ambiguous results will be found, whereas conclusions in agreement with the reference 1PPE spin-polarization data are obtained when considering the spin polarization in accordance with the maximum intensity of the IP peak (i.e. at resonance). This behaviour can be explained taking into account the characteristic resonant behaviour of the $d \rightarrow$ IP excitation pathway. A specific photon energy and IP state level determine the initial d-band energy levels from which the spin-polarized electrons observed at the final state energy may originate. For the Cs-dependent measurements, the central photon energy of $h\nu = 3.05$ eV was chosen to favour the excitation of electrons from the upper Δ_7^5 band at the clean surface, leading to a positive spin polarization at resonance (compare figures 1(a) and (b) above with figures 3 and 4 in [11]). By moving the IP state energy level to lower values under Cs adsorption, the relevant initial d-band level in the two-photon resonance to the IP state is moved accordingly also to lower values. Under continued Cs adsorption and for the same central photon energy, this eventually tunes the resonance to the lower Δ_6^5 states, from which electrons of the opposite spin polarization are preferentially excited. In this way, the spin-polarized electrons excited to the final state energy at the resonance peak are selected in turn from the upper Δ_7^5 to the lower Δ_6^5 states, as would be the case in nonresonant 1PPE measurements with three times the photon energy used for 3PPE. Away from the resonance peak, which defines a dominating excitation pathway, the interpretation of the measured spin polarization is more complicated because of the presence of several excitation pathways that are off-resonant to varying degrees. As we have shown before, both the Δ_7^5 and the Δ_6^5 d-bands can be two-photon-coupled to the IP state by different photon energies [18]. In addition to the resonance favoured at the central photon energy $h\nu = 3.05$ eV employed for the Cs-dependent measurements, a second resonance is possible for higher photon energies. This additional higher-energy resonance would excite spin-polarized electrons from the *lower* Δ_6^5 d-band states to *higher* final state energies, whereas the electrons from the *higher* Δ_7^5 band will appear at *lower* final states for the lower-energy resonance (compare with figures 1(a)). This means that, in contrast to the conditions in the 1PPE measurements, the spin polarization observed in the final states off-resonance in 3PPE cannot be pictured as a simple linear translation from the initial states upwards by the photon energy. Due to the finite excitation bandwidth (170 meV at $h\nu = 3.07$ eV) of the laser pulses, we will have a mixture of two types of spin-polarized contributions as we move away from the resonance peak: the first contribution is related to off-resonant excitation from the upper Δ_7^5 d-band (lower photon energies in the pulse, ω_2 in figure 1(a)), and the second contribution originates from off-resonant excitation from the lower Δ_6^5 d-band by the alternative resonance for higher photon energies (ω_1 in figure 1(a)). According to this interpretation, the additional off-resonant contribution of the ω_1 pathway at the clean surface and low Cs coverages should be reduced with increasing Cs coverage because tuning the IP state to lower energies will tend to suppress any higher photon energy resonance with the lower Δ_6^5 states. This is supported by the observation that the shape of the spin-polarization spectrum off-resonance in the lower panel of figure 4 is beginning to look more similar to the 1PPE curve shown in figure 6(a). In higher-resolution 3PPE experiments [18], the

separate resonances of the IP state with each SO-split initial state are manifest as a clear splitting in the 3PPE IP state peak. In the present investigation, the lower energy resolution necessary to increase the count rate for spin-resolved detection does not allow us to resolve the IP peak fine structure, yet the peculiar signatures of the resonant and off-resonant behaviour are observable in the spin-polarized measurements. The additional information carried by the electron spins therefore provides information about the electron excitation pathways involved that would not be available in the non-spin resolved spectra.

We point out that it is in principle possible, in the Cu(001) system, to also access the d-band spin polarization via a multi-photon excitation process that is nonresonant via the IP state. After deposition of a larger amount of $\approx$0.09 ML Cs on the surface, the workfunction decreases enough to allow the direct observation of the d-band states near the X point in 2PPE [33]. The spin polarization spectrum as a function of the initial state energy deduced by a single 2PPE measurement under these conditions is reported as the solid black line in figure 6(a) ($h\nu = 3.14$ eV, $T = 120$ K). The data, besides a total reduction that is ascribable to an unpolarized background, match the spectral structure of the 1PPE results well. This occurs because the 2PPE excitation pathway on Cs/Cu(001) does not provide the very k-selective resonant conditions that occur in 3PPE through the IP state. We can expect only a spectrally smooth contribution to the observed transitions caused by the unoccupied sp-bands. Such conditions cannot emphasize the contribution of one of the SO-split initial bands like in the resonant 3PPE transitions. This accounts for the overall good agreement of the spin-resolved 2PPE data from Cs/Cu(001) with the (non-resonant) 1PPE data.

5. Summary

In summary, we have investigated different mechanisms of modifying the spin polarization of photoemitted electrons that were optically excited via unoccupied states on the Cu(001) surface. We exploited the coupling of the unoccupied IP states to the occupied SO-split d-bands via circularly polarized multi-photon excitation. We addressed the effects of a controlled modification of the energy levels involved in the multi-photon process. This was achieved either by Cs deposition to lower the vacuum level relevant to the IP or by exploiting the $k_{\parallel}$ dispersion of the states involved. The deposition of a small amount of Cs on Cu(001) has been observed to induce a sign reversal of the spin polarization of the $n = 1$ IP state mediated by the decrease in its energy level, whereas the variation in spin polarization for off-normal photoemission is ascribed to the superimposed contribution of electronic effects and of the measurement geometry.

In addition, our results highlight the important differences between resonant and nonresonant excitation pathways in determining the resulting spin polarization. Furthermore, our investigation illustrates the usefulness of the spin degree of freedom of excited electrons to obtain information about the buildup and decay of excited electron populations on nonmagnetic surfaces.

Acknowledgments

The authors acknowledge F Helbig for valuable technical assistance. W-CL acknowledges support from the National Science Council of Taiwan under grant numbers NSC 96-2112-M-003-015-MY3.

References

[1] Johnson P D 1997 Spin-polarized photoemission *Rep. Prog. Phys.* **60** 1217–304 doi:10.1088/0034-4885/60/11/002

[2] Dil J H 2009 Spin and angle resolved photoemission on non-magnetic low-dimensional systems *J. Phys.: Condens. Matter* **21** 403001 doi:10.1088/0953-8984/21/40/403001

[3] Eyers A, Schäfers F, Schönhense G, Heinzmann U, Oepen H P, Hünlich K, Kirschner J and Borstel G 1984 Characterization of symmetry properties of Pt(111) electron bands by means of angle-, energy-, and spin-resolved photoemission with circularly polarized synchrotron radiation *Phys. Rev. Lett.* **52** 1559–62 doi:10.1103/PhysRevLett.52.1559

[4] Oepen H P, Hünlich K, Kirschner J, Eyers A, Schafers F, Schönhense G and Heinzmann U 1985 Experimental symmetry analysis of energy bands near critical points in Pt using spin- and momentum-resolved photoemission *Phys. Rev.* B **31** 6846–8 doi:10.1103/PhysRevB.31.6846

[5] Garbe J, Venus D, Suga S, Schneider C and Kirschner J 1986 Spin-polarized angle-resolved photoemission from the (110) surface of platinum *Surf. Sci.* **178** 342–8 doi:10.1016/0039-6028(86)90310-9

[6] Müller N, Kessler B, Schmiedeskamp B, Schönhense G and Heinzmann U 1987 Spin-resolved photoemission from Ir(111): transitions into a secondary band and energetic position of the final state bands *Solid State Commun.* **61** 187–92 doi:10.1016/0038-1098(87)90027-5

[7] Heinzmann U 1987 Angle-, energy- and spin-resolved photoelectron emission using circularly polarized synchrotron radiation *Phys. Scr.* **T17** 77–88 doi:10.1088/0031-8949/1987/T17/009

[8] Garbe J and Kirschner J 1989 Spin-dependent photoemission intensities from platinum (111) *Phys. Rev.* B **39** 9859–64 doi:10.1103/PhysRevB.39.9859

[9] Schneider C M, Garbe J, Bethke K and Kirschner J 1989 Symmetry-dependent alignment of the electron-spin polarization vector due to electronic band hybridization observed in photoemission from Ag(100) *Phys. Rev.* B **39** 1031–5 doi:10.1103/PhysRevB.39.1031

[10] Schneider C M, Demiguel J J, Bressler P, Schuster P, Miranda R and Kirschner J 1990 Spin- and angle-resolved photoemission from single crystals and epitaxial films using circularly polarized synchrotron radiation *J. Electron. Spectrosc. Relat. Phenom.* **51** 263–74 doi:10.1016/0368-2048(90)80157-6

[11] Winkelmann A, Bisio F, Ocana R, Lin W-C, Nývlt M, Petek H and Kirschner J 2007 Ultrafast optical spin injection into image-potential states of Cu(001) *Phys. Rev. Lett.* **98** 226601 doi:10.1103/PhysRevLett.98.226601

[12] Winkelmann A, Lin W-C, Bisio F, Petek H and Kirschner J 2008 Interferometric control of spin-polarized electron populations at a metal surface observed by multiphoton photoemission *Phys. Rev. Lett.* **100** 206601 doi:10.1103/PhysRevLett.100.206601

[13] Aeschlimann M, Bauer M, Pawlik S, Weber W, Burgermeister R, Oberli D and Siegmann H C 1997 Ultrafast spin-dependent electron dynamics in fcc Co. *Phys. Rev. Lett.* **79** 5158–61 doi:10.1103/PhysRevLett.79.5158

[14] Schmidt A B, Pickel M, Wiemhofer M, Donath M and Weinelt M 2005 Spin-dependent electron dynamics in front of a ferromagnetic surface *Phys. Rev. Lett.* **95** 107402 doi:10.1103/PhysRevLett.95.107402

[15] Weinelt M, Schmidt A B, Pickel M and Donath M 2007 Spin-polarized image-potential-state electrons as ultrafast magnetic sensors in front of ferromagnetic surfaces *Prog. Surf. Sci.* **82** 388–406 doi:10.1016/j.progsurf.2007.03.010

[16] Bisio F, Nývlt M, Franta J, Petek H and Kirschner J 2006 Mechanisms of high-order perturbative photoemission from Cu(001) *Phys. Rev. Lett.* **96** 087601 doi:10.1103/PhysRevLett.96.087601

[17] Winkelmann A, Hartung D, Engelhard H, Chiang C-T and Kirschner J 2008 High efficiency electron spin polarization analyzer based on exchange scattering at Fe/W(001) *Rev. Sci. Instrum.* **79** 083303 doi:10.1063/1.2949877

[18] Winkelmann A, Lin W-C, Chiang C-T, Bisio F, Petek H and Kirschner J 2009 Resonant coherent three-photon photoemission from Cu(001) *Phys. Rev.* B **80** 155128 doi:10.1103/PhysRevB.80.155128

[19] Eckardt H, Fritsche L and Noffke J 1984 Self-consistent relativistic band structure of the noble metals *J. Phys. F: Met. Phys.* **14** 97–112 doi:10.1088/0305-4608/14/1/013
[20] Weinelt M 2002 Time-resolved two-photon photoemission from metal surfaces *J. Phys.: Condens. Matter* **14** R1099–141 doi:10.1088/0953-8984/14/43/202
[21] Thörner G, Borstel G, Dose V and Rogozik J 1985 Unoccupied electronic surface resonance at Cu(001) *Surf. Sci.* **157** L379–83 doi:10.1016/0039-6028(85)90667-3
[22] Kuch W and Schneider C M 2001 Magnetic dichroism in valence band photoemission *Rep. Prog. Phys.* **64** 147–204 doi:10.1088/0034-4885/64/2/201
[23] Hanuschkin A, Wortmann D and Blügel S 2007 Image potential and field states at Ag(100) and Fe(110) surfaces *Phys. Rev.* B **76** 165417 doi:10.1103/PhysRevB.76.165417
[24] Echenique P M and Pendry J B 1978 The existence and detection of Rydberg states at surfaces *J. Phys. C: Solid State Phys.* **11** 2065–75 doi:10.1088/0022-3719/11/10/017
[25] Papageorgopoulos C A 1982 Studies of separate adsorption and coadsorption of Cs and $O2$ on Cu(100) *Phys. Rev.* B **25** 3740–9 doi:10.1103/PhysRevB.25.3740
[26] Arena D A, Curti F G and Bartynski R A 1997 Unoccupied electronic states of the Cs/Cu(100) and Cs/Cu(111) adsorption systems *Phys. Rev.* B **56** 15404–11 doi:10.1103/PhysRevB.56.15404
[27] Lang N D and Kohn W 1973 Theory of metal surfaces: induced surface charge and image potential *Phys. Rev.* B **7** 3541–50 doi:10.1103/PhysRevB.7.3541
[28] Soukiassian P, Riwan R, Lecante J, Wimmer E, Chubb S R and Freeman A J 1985 Adsorbate-induced shifts of electronic surface states: Cs on the (100) faces of tungsten, molybdenum and tantalum *Phys. Rev.* B **31** 4911–23 doi:10.1103/PhysRevB.31.4911
[29] Binnig G, Frank K H, Fuchs H, Garcia N, Reihl B, Rohrer H, Salvan F and Williams A R 1985 Tunneling spectroscopy and inverse photoemission: image and field states *Phys. Rev. Lett.* **55** 991–4 doi:10.1103/PhysRevLett.55.991
[30] Bisio F, Winkelmann A, Lin W-C, Chiang C-T, Nývlt M, Petek H and Kirschner J 2009 Band structure effects in surface second harmonic generation: the case of Cu(001) *Phys. Rev.* B **80** 125432 doi:10.1103/PhysRevB.80.125432
[31] Palik E D (ed) 1991 *Handbook of Optical Constants of Solids I* (New York: Academic)
[32] Azzam R M A and Bashara N M 1992 *Ellipsometry and Polarized Light* 3rd ed. (Amsterdam: North-Holland)
[33] Petek H, Nagano H and Ogawa S 1999 Hole decoherence of d bands in copper *Phys. Rev. Lett.* **83** 832 doi:10.1103/PhysRevLett.83.832